Transfer-matrix formulation of field-assisted tunneling

C. Pérez del Valle,[1] R. Lefebvre,[1,2] and O. Atabek[1]
[1]*Laboratoire de Photophysique Moléculaire, Campus d'Orsay, 91405 Orsay, France*
[2]*UFR de Physique Fondamentale et Appliquée, Université Pierre et Marie Curie, 75231 Paris, France*
(Received 23 June 1998; revised manuscript received 14 September 1998)

A transfer-matrix technique is formulated to treat the scattering of a particle incident on a piecewise constant potential and interacting with an oscillatory field. A study of tunneling through a single barrier shows in the transmission probabilities, for absorption or emission of quanta from the field, replicas below the barrier of the overbarrier field-free transmissivity, with its resonant structure. In the case of resonant tunneling through a double barrier, an appropriate choice of parameters gives evidence for a change in the regime, with inhibition of transmission at a resonance energy of the intermediate well when the period of the field approaches the lifetime of the resonant state. The technique can be extended to treat scattering of a particle by more general potentials in the presence of an oscillatory perturbation. As an illustrative example, the transmissivity as a function of a bias potential in a double-barrier structure is calculated. [S1050-2947(99)00405-9]

PACS number(s): 33.80.−b, 73.40.Gk, 73.20.Dx

I. INTRODUCTION

The transmissivity of a particle incident on one or more barriers and interacting with a time-periodic external field is of interest for the understanding of many physical processes, such as field emission, tunneling chemical reactions, or transmission through semiconductor double-barrier structures. The problem has been treated with a large variety of models and methods. We review only some papers which are close to the present approach. Sokolovski and Yu [1] and Sokolovski [2,3] have applied a semiclassical procedure to obtain the total transmissivity through a double barrier in the presence of a harmonic perturbation. This situation gives rise to the well-known resonant tunneling effect. In the absence of the perturbation, and if the tunneling probabilities through each of the barriers are identical, unit transmissivity is obtained when the incident energy coincides with an energy of the intermediate well. Sokolovski delineated several regimes from a comparison of the three relevant parameters: Γ^{-1}, the lifetime of the particle trapped in the well with energy $E_R - i\Gamma/2$,ω^{-1}, proportional to the period of the field; and W, which measures the coupling of the particle to the field. When W and Γ are both smaller than ω, a structure appears in the transmissivity, with peaks separated by ω. A simple explanation is that the particle can tunnel through the double-barrier device if, by absorption or emission of field quanta, its energy fulfills the resonant condition. A drastic change occurs in the transmissivity when ω is of the order or smaller than Γ while W is larger than both ω and Γ. The transmissivity is peaked at energies $E_R \pm W$. The interpretation is based on an adiabatic picture. With a low field frequency the particle ''sees'' a time-dependent double barrier and an efficient transmissivity occurs only at the turning points of the barrier motion.

In a series of papers Azbel [4–6] and Azbel and Tsukernik [7] consider resonant tunneling in the presence of a time-dependent perturbation having a spatial dependence involving a δ function of position. This form of the interaction allows extensive analytical derivations and applications even to complicated structures. Conditions for activation of the transmission through a barrier are established within this model. The adiabatic regime corresponds to the particle following a time-dependent eigenstate until its energy reaches the top of the barrier.

Time-dependent barriers have also been considered by Büttiker and Landauer [8] to test various proposals for the definition of tunneling traversal times. They stress the multiquantum aspect of the scattering and propose a semiclassical approach to calculate the scattering amplitudes. A related subject is the observation of replicas of the main feature in phonon-assisted [9] or plasmon-assisted [10] tunneling in double-barrier semiconductor structures. Theoretical treatments of these effects based on a second-quantization formalism rather than a time-dependent formulation have been proposed [11,12]. The explanation of the replica phenomenon is that by emission of a quantum the incident electron reaches the energy that favors efficient transmissivity through the structure.

The work that is closest to the present approach is that of Sacks and Szöke [13]. They provide exact results for the reflection and transmission coefficients of a number of stepwise constant potentials for an electron interacting with an electromagnetic field of arbitrary intensity. We use their approach to revisit the case of a single barrier and to extend the treatment to the double-barrier situation. We have found it convenient to define in this context a generalized transfer matrix. Such matrices have been widely used for the determination of transmission and reflection amplitudes in a large variety of situations [14–17]. They are generally of dimension 2, since at every junction between two regions there is, in the absence of a time-dependent perturbation, only one incident wave and one reflected wave on each side of the junction. In the present case, at every discontinuity of the potential, there are, in principle, an infinite number of incident and reflected waves, since an arbitrary number of quanta can be exchanged by the particle and the field. Convergence with respect to the number of channels must be checked. An advantage of the transfer matrix is that it can be used even in the case of an arbitrary potential, since any potential can be considered as the limit of an infinite number of steps of van-

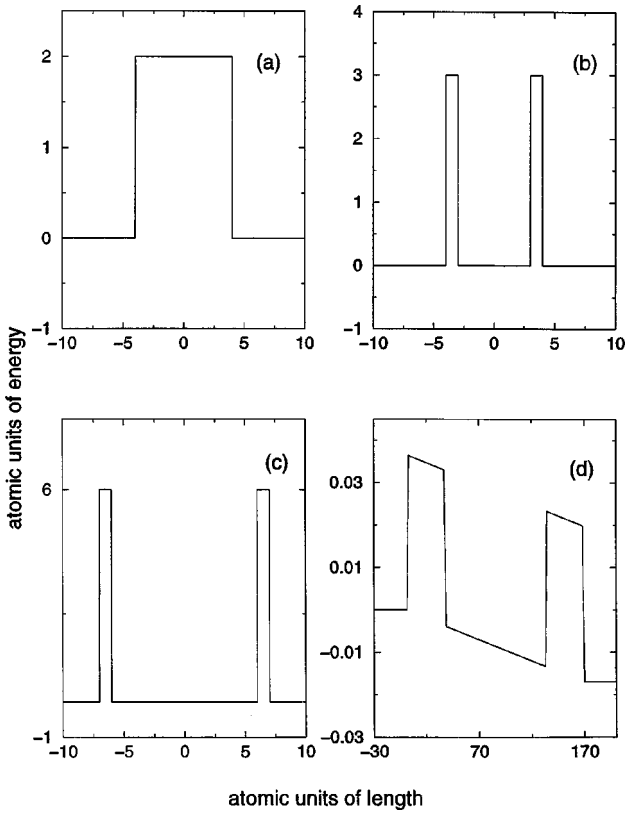

FIG. 1. The different potential arrangements considered in the paper. (a) the rectangular barrier of Sec. III; (b) and (c) two double-barrier structures examined in Sec. IV; (d) a double barrier with an applied electric field of 10^{-4} a.u. studied in Sec. V. This corresponds to a bias voltage of 0.46 V.

ishing widths [18]. We will also make use of this capacity of the method.

Section II describes the transfer matrix which takes into account the multiquantum aspect of the scattering of a particle incident on the discontinuities present in a stepwise constant potential. The final reflection and transmission amplitudes are derived from an overall transfer matrix taking into account all successive scattering events. The various potential arrangements to which the method is applied are shown in Fig. 1. Tunneling through a single barrier is treated in Sec. III. The multiquantum aspect of field-assisted processes is stressed. Each peak in the transmissivity has contributions from several multiphoton processes with a clear interpretation in terms of virtual and real exchanges of energy between the particle and the field at the two potential discontinuities. In Sec. IV we consider the double-barrier structure which is one of the basic models in semiconductor research. Although we do not consider at this point any bias of the potential, the model is rich enough to investigate carefully the roles played by the competing different time scales which were identified in previous approximate treatments [1–3]. Finally Sec. V considers application of the method to a potential of a more complex shape: a biased double-barrier structure, with therefore consideration of both static and oscillatory electric fields. Transfer matrices have to be evaluated at all the points retained in the numerical representation of the potential.

We recall [14,19] that the transmissivity of the one-dimensional (1D) arrangement allows for the calculation of the tunneling current under the assumption of conservation of the transverse components of the energy and momentum of the incident electron in the analysis of the 3D situation. The current has two opposing contributions (from left to right and from right to left). Integration over the transverse components of the wave-vector leads for the current to a 1D integral over the longitudinal component of the energy, with the 1D transmissivity under the integral sign (the so-called Tsu-Esaki formula [14]).

II. TRANSFER MATRICES AT POTENTIAL DISCONTINUITIES

The discussion is patterned after that valid for the field-free case [14,16–18]. The main change is that the transfer matrix has, in principle, infinite dimension, so that truncation and convergence tests are necessary.

In velocity gauge, in one dimension, the wave equation for a particle of unit charge coupled to a field is in atomic units [13],

$$i\frac{\partial}{\partial t}\psi(x,t)=\left(-\frac{1}{2m}\frac{\partial^2}{\partial x^2}-\frac{A(t)p_x}{m}+V(x)\right)\psi(x,t). \quad (1)$$

The mass m is in units of the free electron mass. $V(x)$ is the potential energy. The potential vector is supposed to be spatially invariant on the length scale of interest. It is written $A_0\cos(\omega t)$ so that the associated electric field is $E_0\sin(\omega t)$, with $E_0=\omega A_0 . p_x$ is the linear momentum $-i\partial/\partial x$. In a region of constant potential V the solutions are Gordon-Volkov waves

$$\psi(x,t)=\exp\left[i\left(\pm kx-Et\pm\frac{A_0k\sin(\omega t)}{m\omega}\right)\right], \quad (2)$$

with $k=[2m(E-V)]^{1/2}$.

Let X_i be the position of the ith discontinuity of the potential. If N is taken as the maximum number of quanta that can be exchanged (either by absorption or emission) by the particle and the field as a result of the scattering by the complete potential arrangement, the wave function either to the left (L) and to the right (R) of X_i is written as a combination of Gordon-Volkov waves traveling in both directions,

$$\Psi^L(x,t)=\sum_{n=-N}^{n=N}t_n^L\exp\left[i\left(k_n^Lx-E_nt+\frac{A_0k_n^L\sin(\omega t)}{m\omega}\right)\right]+r_n^L\exp\left[-i\left(k_n^Lx+E_nt+\frac{A_0k_n^L\sin(\omega t)}{m\omega}\right)\right], \quad (3)$$

$$\Psi^R(x,t)=\sum_{n=-N}^{n=N}t_n^R\exp\left[i\left(k_n^Rx-E_nt+\frac{A_0k_n^R\sin(\omega t)}{m\omega}\right)\right]+r_n^R\exp\left[-i\left(k_n^Rx+E_nt+\frac{A_0k_n^R\sin(\omega t)}{m\omega}\right)\right]. \quad (4)$$

E_n is $E+n\omega$, E being the initial energy of the particle. If V^L and V^R are the potential values on the left and on the right of X_i, the wave numbers present in these wave functions are to be calculated as

$$k_n^{L,R}=[2m(E_n-V^{L,R})]^{1/2}. \tag{5}$$

The sign of $E_n-V^{L,R}$ determines the open or closed character of channel n. The positive determination of the square root ensures the correct behavior of the nth component of the wave function. k_n is $i\kappa_n$, with κ_n positive. This can be checked at a junction between a classical and a nonclassical region. A wave travelling to the right (i.e., multiplied by an amplitude t_n^R) should behave as $\exp[-\kappa x]$. A wave travelling to the left behaves as $\exp[+\kappa x]$. The total number of amplitudes in any region (between two discontinuities) is $2(2N+1)$. The two wave functions and their derivatives are to be matched at the discontinuity X_i *at all times* [13]. We have to find some way to calculate the amplitudes t_n^R and r_n^R from the knowledge of t_n^L and r_n^L (with the usual convention of a propagation from left to right). The wave function is Fourier expanded with the help of the identity:

$$\exp\left(\pm i\frac{A_0k_n}{m\omega}\sin(\omega t)\right)=\sum_{p=-\infty}^{p=+\infty}J_p\left(\pm\frac{A_0k_n}{m\omega}\right)\exp(ip\omega t). \tag{6}$$

By limiting p to go from $-N$ to $+N$ and equating the coefficients on both sides of the same Fourier component one gets a number of equations $[2(2N+1)]$ giving the t_n^R's and the r_n^R's in terms of the t_n^L's and the r_n^L's. Introducing two column vectors

$$\mathbf{a}^L=\begin{pmatrix} t_{-N}^L \\ \cdot \\ t_0^L \\ \cdot \\ t_N^L \\ r_{-N}^L \\ \cdot \\ r_0^L \\ \cdot \\ r_N^L \end{pmatrix}, \quad \mathbf{a}^R=\begin{pmatrix} t_{-N}^R \\ \cdot \\ t_0^R \\ \cdot \\ t_N^R \\ r_{-N}^R \\ \cdot \\ r_0^R \\ \cdot \\ r_N^R \end{pmatrix}, \tag{7}$$

the matching condition is now written in matrix form

$$\mathbf{M^L}(X_i)\mathbf{a^L}=\mathbf{M^R}(X_i)\mathbf{a^R}, \tag{8}$$

where the matrices $\mathbf{M^{L,R}}(X_i)$ are given by the equation

$$\mathbf{M}(X_i)=\begin{pmatrix} \cdots & \exp[ik_nX_i]J_p(A_0k_n/m\omega) & \cdots & \exp[-ik_nX_i]J_p(-A_0k_n/m\omega) & \cdots \\ \cdots & \cdots & \cdots & \cdots & \cdots \\ \cdots & k_n\exp[ik_nX_i]J_p(A_0k_n/m\omega) & \cdots & -k_nexp[-ik_nX_i]J_p(-A_0k_n/m\omega) & \cdots \end{pmatrix} \tag{9}$$

calculated with either the k_n^L's or the k_n^R's. The left half of the matrix is made of the coefficients of the Fourier components of the transmitted waves (upper part) and their derivatives (lower part), while the right half comes from the reflected waves. n is the index of a transmission or reflection amplitude, while p is the index of a Fourier component.

From Eq. (8) we obtain

$$\mathbf{a^R}=[\mathbf{M^R}(X_i)]^{-1}\mathbf{M^L}(X_i)\mathbf{a^L}=\mathcal{M}(X_i)\mathbf{a^L}. \tag{10}$$

This relation defines the transfer matrix $\mathcal{M}(X_i)$ to pass the discontinuity at position X_i. Let us consider now a general situation with discontinuities at positions $X_1, X_2, \ldots, X_P$. Calling $\mathbf{a}^{\text{in}}$ the vector of amplitudes in the potential-free region on the left and $\mathbf{a}^{\text{out}}$ the vector of amplitudes in the right potential-free region, we can write

$$\mathbf{a}^{\text{out}}=\mathcal{M}(X_1)\mathcal{M}(X_2)\cdots\mathcal{M}(X_P)\mathbf{a}^{\text{in}}. \tag{11}$$

Although there are $4(2N+1)$ amplitudes in these $2(2N+1)$ equations, once we introduce the usual scattering conditions, the number of unknowns become equal to the number of equations. In the vector $\mathbf{a}^{\text{in}}$ only t_0 is kept and made equal to 1. In the vector $\mathbf{a}^{\text{out}}$, all the amplitudes r_n are taken equal to zero. The equations determine the $2N+1$ amplitudes for reflection to the left and the $2N+1$ amplitudes for transmission to the right.

A final comment on this technique: it is possible to deconnect [13] the number of amplitudes and the number of Fourier components when going to higher intensities of the field. If the number of Fourier components exceeds the number of Gordon-Volkov waves, the number of equations becomes larger than the number of unknowns. A least-squares procedure allows to define a square transfer matrix even in such a case and to overcome the numerical difficulties associated with the inversion of large and ill-conditioned matrices.

III. REPLICAS OF BARRIER RESONANCE STRUCTURE

The transmissivity of the rectangular barrier is determined in all introductory books on quantum mechanics (see, for instance, Merzbacher [20]). It is characterized by oscillations at energies above the barrier top which are due to constructive interference produced by the reflections taking place at the two discontinuities of the potential. We examine now the effect of a coupling with an oscillatory field. The barrier is such that very little transmissivity is allowed below the top in order to see clearly the effects of the perturbation. The

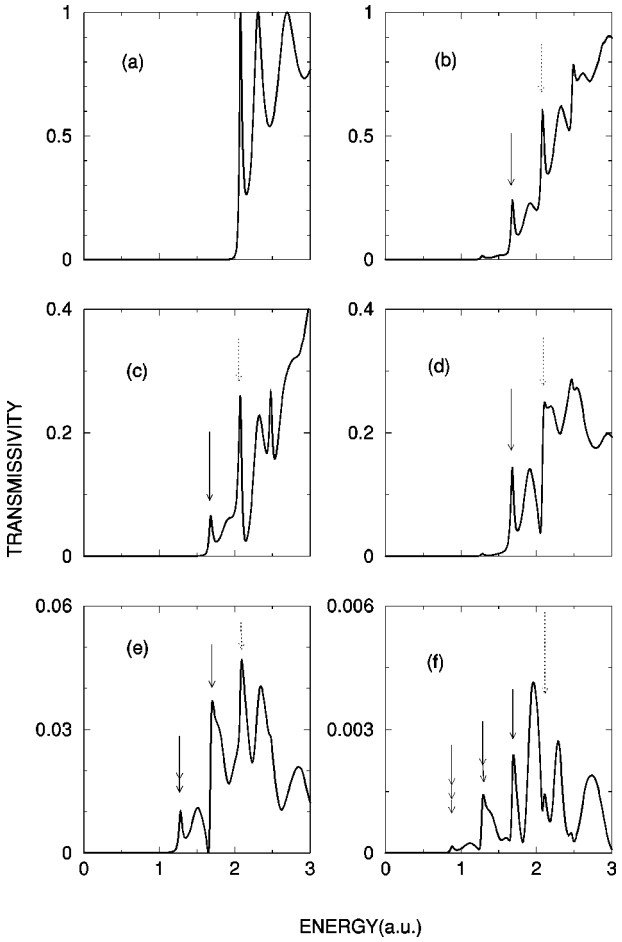

FIG. 2. Replicas of overbarrier structure of the tranmissivity produced by the coupling of an electron to an oscillating electric field of amplitude 0.1 a.u. The parameters of the barrier [cf. Fig. 1(b)] are in a.u.: 8 for the width, 2 for the height. The frequency of the field is $\omega=0.4$ a.u. (a) the field-free transmissivity showing the first two resonances above the barrier. (b) The total transmissivity in the presence of the field. (c)–(f) The transition probabilities for absorption of zero, one, two, and three photons. The dotted vertical arrow indicates the position of the first overbarrier resonance. The one-, two-, and three-headed solid arrows display the positions of below-barrier replicas of this resonance shifted by one, two, and three quanta. There is clear evidence that the overbarrier structure is translated into an underbarrier structure of the same shape.

parameters in atomic units are: 1 for the mass, 8 for the barrier width a, and 2 for the barrier height V_0. The barrier is depicted in Fig. 1(a). The field-free transmissivity up to 3 a.u. is shown in Fig. 2(a). It shows a pronounced resonant structure above the barrier maximum.

The particle is now coupled to an electric field of maximum amplitude E_0 equal to 0.1 a.u. The frequency is $\omega=0.4$ a.u. The determination of N (maximum number of effectively exchanged quanta) is made by requiring the fulfillment of the rule

$$\sum_{n=N_1}^{n=+N} R_n+\sum_{n=N_2}^{n=+N} T_n=1. \tag{12}$$

In this equation N_1 is the index of the lowest channel open for reflection (i.e., the first channel with a real wave number in the left asymptotic region) and N_2 the corresponding index for transmission (first channel with a real wave number in the right asymptotic region). R_n and T_n are the transition probabilities for reflection or transmission with absorption (emission) of n quanta. They are obtained from the amplitudes r_n and t_n by the relations

$$R_n=\left|\frac{k_n^{\mathrm{in}}}{k_0}\right||r_n^{\mathrm{in}}|^2, \quad T_n=\left|\frac{k_n^{\mathrm{out}}}{k_0}\right||t_n^{\mathrm{out}}|^2, \tag{13}$$

with $k_0=[2mE]^{1/2}$. Table I shows how the rule given in Eq. (12) is progressively fulfilled in this example. The energy is that of the first resonance in the field-free transmissivity ($E=2.07$ a.u.). $N=8$ can be considered as giving accurate results.

TABLE I. Convergence to the fulfillment of the condition on the sum of reflection and transmission probabilities [Eq. (12)]. This series of calculations is performed at an energy $E=2.07$ a.u., in the neighborhood of the first resonance of the barrier shown as Fig. 1(a) and studied in Fig. 2, with the same parameters for the field. R_T is the total reflection probability and T_T the total transmission probability. N is the maximum number of exchanged quanta kept in the expression of the wave function [cf Eq. (7)]. $N=0$ corresponds to the field-free case.

N	R_T	T_T	R_T+T_T
0	0.130 890 7	0.869 109 30	1.000 000 0
1	0.669 104 30	0.506 188 32	1.175 292 6
2	0.509 509 77	0.523 219 60	1.032 272 9
3	0.501 754 77	0.504 865 94	1.006 620 7
4	0.494 172 46	0.506 121 72	1.000 294 2
5	0.494 295 80	0.505 742 23	1.000 038 0
6	0.494 292 00	0.505 716 48	1.000 008 5
7	0.494 284 77	0.505 715 74	1.000 000 5
8	0.494 284 40	0.505 715 63	1.000 000 0

Figure 2 gives the total transmissivity (b), but also in (c)–(f) the transition probabilities T_0, T_1, T_2, and T_3 for absorption of 0, 1, 2, and 3 quanta. The transition probabilities T_{-1}, T_{-2}, and T_{-3} for emission of 1,2, and 3 quanta are not shown. They are identical, except for a shift, to the absorption probabilities, according to the general rules

$$R_n(E)=R_{-n}(E+n\omega), \quad T_n(E)=T_{-n}(E+n\omega). \tag{14}$$

These relations express the equality of probabilities when the initial and final states are permuted. They apply to symmetric potential arrangements. We now concentrate on the role of the first two resonances of the field-free case, say with energies E_R^1 and E_R^2. The total transmission probability shows clearly that the structure occurring above the barrier is now also present below it. The peaks are occurring as expected at energies $E_R^1-\omega$ and $E_R^2-\omega$. The spectrum is an exact *replica* of the field-free transmission. There is even a weaker replica at energies $E_R^1-2\omega$ and $E_R^2-2\omega$. Figure 2(c) shows T_0. The same feature is present, but since there is no net absorption or emission of photons, a two-photon process must be invoked: the particle incident at energy $E_R^i-\omega$, with $i=1,2$, absorbs a quantum when meeting the left edge of the barrier and emits a quantum when meeting the right edge.

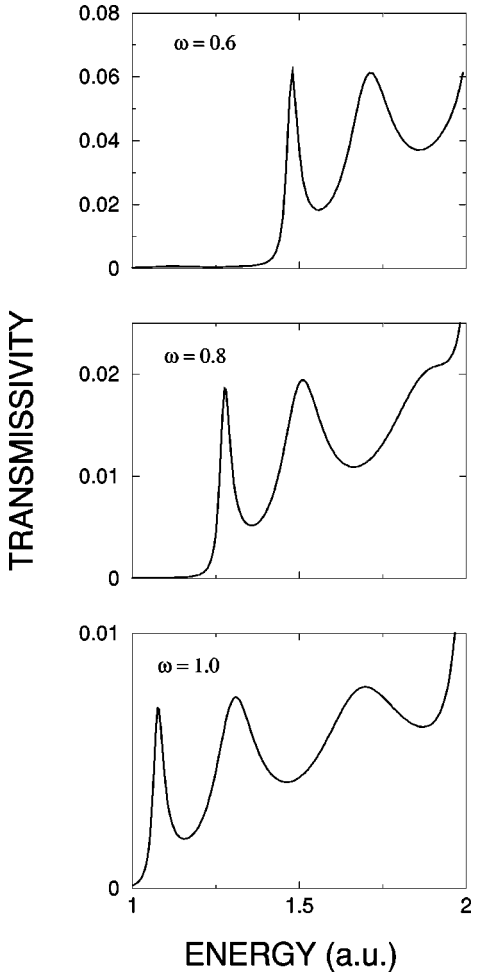

FIG. 3. Effect of a change of frequency on the replicas of a rectangular barrier. The barrier parameters are those used for Fig. 2. As the frequency ω increases a replica of the third overbarrier resonance appears in the total transmissivity below the top energy of the barrier (2 a.u. in the present case). The replicas are essentially associated with a T_1 process: absorption of 1 photon at the first discontinuity of the potential gives to the particle an energy in coincidence with one of the resonances above the barrier.

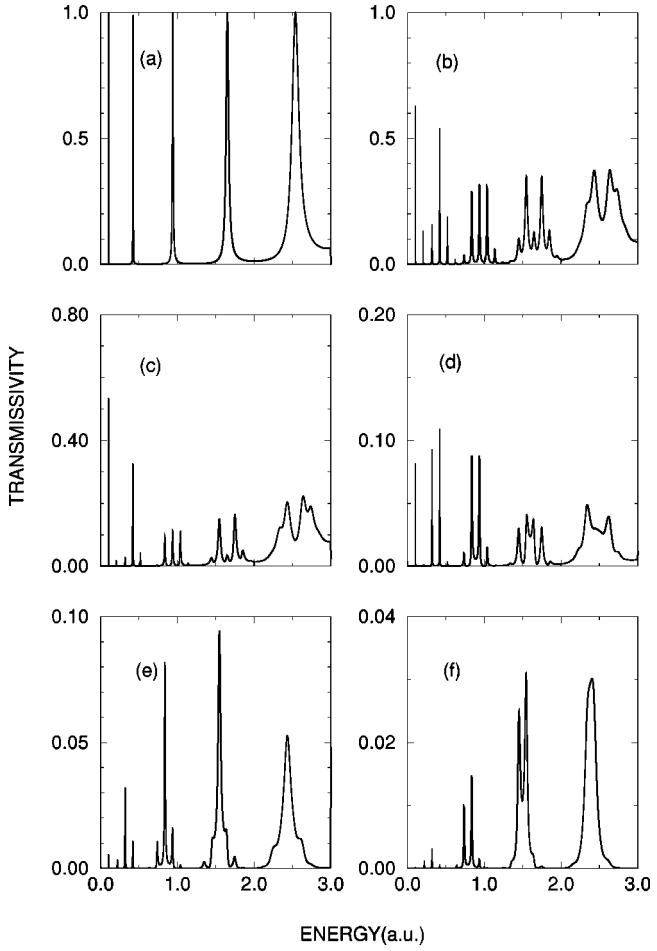

FIG. 4. Transmission through a double-barrier potential [Fig. 1(b)] in the presence of an oscillatory electric field of amplitude 0.01 a.u. Each of the barriers has a width of 1 a.u. and a height of 3 a.u. The well between the barriers has a width of 6 a.u. The frequency ω is 0.1 a.u. (a) The field-free transmissivity displaying the five resonances created by the well; (b) the total transmissivity showing the multiplets created by each resonance (note the change in the structure of the multiplets as one goes to resonances of increasing width); (c)–(f) the probabilities for absorption of zero, one, two, and three photons. T_0 (c) is similar to the total transmissivity (b), but reduced in scale. Processes with absorption or emission of photons contribute significantly to the tranmission.

We now go to Fig. 2(d), which shows that it is T_1 that most contributes to the replica. The process is a single-photon one. The particle incident at energy $E_R^i-\omega$ absorbs a photon to reach the doorway. This is the situation which comes immediately to mind if one thinks of photon-assisted transmission. However, we observe that not all of the replica is due to this one-photon mechanism. In T_2 [Fig. 2(e)] a replica is also present, now at energies $E_R-2\omega$. A two-photon process is involved, the absorption occurring on the left edge of the barrier. The explanation is the same for T_3, with now implication of three quanta. However, the probability has dropped considerably.

Similar calculations made with lower electric field amplitudes at the same frequency ($\omega=0.4$ a.u.) show that the replicas are reduced. When the frequency is increased, while the field amplitude is maintained at the value 0.1 a.u., the replicas are displaced to lower energies. This is shown in Fig. 3. The replica of the third overbarrier appears clearly now for $\omega>0.8$ a.u. The amplitudes of the replicas are reduced. This is expected, since in a multichannel Floquet picture, the threshold intervals are increased, while the interchannel couplings are maintained constant.

IV. ANALYSIS OF MULTIPLET STRUCTURE IN RESONANT DOUBLE BARRIER TUNNELING

It is possible to choose the parameters of a double-barrier structure to produce a wide variation of the resonance widths associated with the unstable states of the intermediate well. The resonance width is one of the key parameters to understand the effect of a time periodic perturbation [2,3] on the transmission pattern. Figure 4 shows in (a) the field-free transmission through the double-barrier of Fig. 1(b). It is made of two identical barriers of width 1 a.u., of height 3 a.u., with the intermediate well extending over 6 a.u. There are five resonances below the potential maximum, with widths from ~ 0.0005 a.u. for the narrowest to 0.0518 a.u.

for the broadest one. Figure 4(b) gives the total transmissivity for a field of maximum amplitude $E_0=0.01$ a.u. and of frequency $\omega=0.1$ a.u. One recognizes easily the different multiplets arising from the successive resonances, with peak to peak separation equal to the frequency. Similar multiplets have been obtained by Sokolovski [3]. Various processes can contribute to a given peak. Consider, for instance, the multiplet associated with the field-free resonance occurring at $E_R=0.941$ a.u. T_0, T_1, T_2, and T_3 are given in Figs. 4(c)–4(f), respectively. Figure 4(c) shows essentially the same pattern as in the total transmissivity, but with a reduction in scale. The central peak in T_0 corresponds to a direct access to the resonant state, while the two peaks at $E_R\pm\omega$ correspond to two-photon processes (one photon is either absorbed or emitted to reach the resonant energy, and then reemitted or reabsorbed). Let us now go to the T_1 or T_{-1} processes. Only T_1 is shown in Fig. 4(d), T_{-1} being identical, except for a shift [cf. Eq. (14)]. The two main peaks are at $E_R-\omega$ and E_R. A reasonable explanation is that in the left peak, absorption of a photon is needed to reach E_R, while in the right peak absorption follows the passage through energy E_R. The peaks in T_{-1} are at energies E_R and $E_R+\omega$. This restores the symmetry in the multiplet, despite the asymmetry of the contributions of both T_1 and T_{-1}. The main peak of T_2 is at energy $E_R-\omega$: absorption of a photon takes place before reaching the doorway energy, absorption of a further photon takes place afterward. In T_{-2} the main peak is at energy $E_R+\omega$. The rule $T_n(E)=T_{-n}(E+n\omega)$ is therefore at the origin of the symmetry of the successive patterns in the total transmissivity, Fig. 4(b).

We turn now to another striking feature of the successive multiplets. There is a progressive change with a decreasing contribution of the central peak. This is strongly reminiscent of the change from a nonadiabatic to an adiabatic regime described by Sokolovski [2,3], this time occurring *in the same spectrum*. The only parameter that changes across the spectrum is the resonance width. We now proceed to a detailed study of the parameters influencing the structure of a given multiplet. We choose to study the resonance with energy $1.651-i0.029$ of the field-free transmissivity. ω is kept equal to 0.1 a.u. and the amplitude of the field is varied. According to Sokolovski, to reach the adiabatic regime, the period of the field should be of the order or longer than the lifetime of the resonant state. We have here $\omega>\Gamma$, which is an obvious condition to observe a structure, and we observe that by increasing the field amplitude the change in the spectrum is very much like that characterizing the adiabatic regime [2]. Figure 5 is showing in (a) an enlarged view of the field-free transmissivity in the region of the resonance. We now switch on a field with amplitudes 0.002, 0.005, 0.01, 0.02, and 0.022 a.u. Only the total transmissivity is shown. There is a drastic change of the shape of the multiplet with the field amplitude. At low field amplitude [Fig. 5(b)] there is a central peak with a width of the same order as the field-free width, with only small changes in the wings of the peak. As the field amplitude increases, the expected multiplet structure develops. However, the central peak loses progressively its intensity. The prominent lateral peaks occur in Fig. 5(d) at $E_R\sim\pm\omega$, in (e) at $E_R\sim\pm2\omega$ and finally, for the last studied intensity, at $E_R\sim\pm3\omega$. This shows that an adiabatic interpretation extends beyond the limit given by Sokolovski

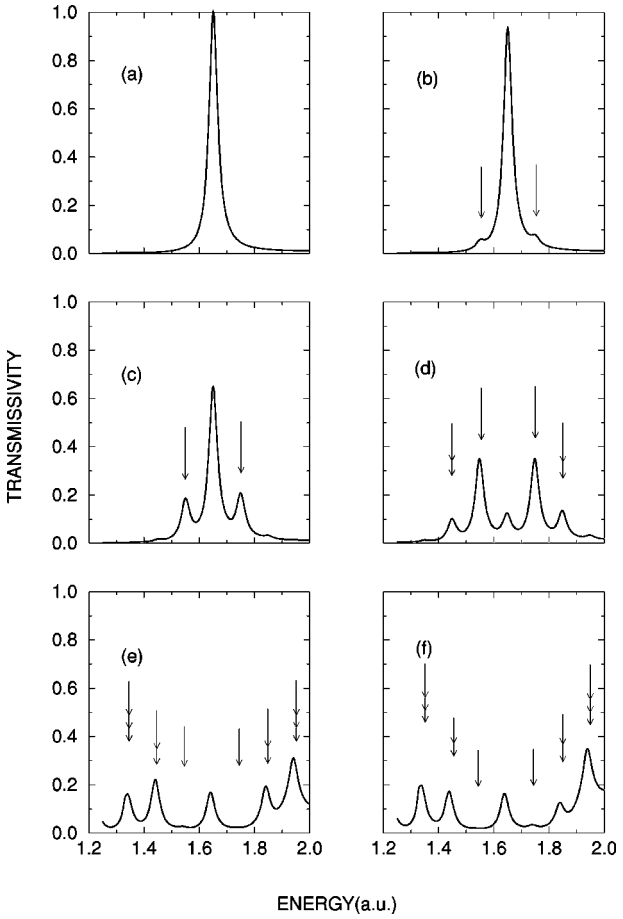

FIG. 5. Effect of electric field amplitude on the shape of a multiplet. The resonance at energy 1.651 a.u. of (a) of Fig. 4 is chosen. The frequency of the field is still $\omega=0.1$ a.u. Only the total transmissivity is shown. (a) The fied-free transmissivity; (b)–(f) spectra for electric field amplitudes equal to 0.002, 0.005, 0.01, 0.02, and 0.03. In (d)–(f) the dominant peaks are at energies approximately equal to $E_R\pm\omega$, $E_R\pm2\omega$, and $E_R\pm3\omega$ respectively. *n*-headed arrows are at positions $E_R\pm n\omega$.

[2,3]. In order to complete the analysis there is to relate the field intensity to a parameter with the dimension of an energy. Since the calculation is done in velocity gauge the coupling cannot be read directly from the wave equation. However, since exchange of energy between the particle and the field takes place only in the region of the double barrier, it is safe to take as a measure of the coupling parameter the product of the electric field amplitude by the total length spanned by the potential structure. This total length being 8 a.u., the coupling parameter, say *W*, is respectively 0.016, 0.04, 0.08, 0.16, and 0.176 a.u. for the spectra of Figs. 5(b)–5(f). The condition $W>\omega$ for a reduction of transmissivity at the resonance energy is thus clearly evidenced by this series. There is a correlation between the position of the lateral peaks and the coupling. This was the essential message of Ref. [2].

We end this discussion by a study of the effect of a change of the frequency ω for a given coupling to the field. Figure 6 is built like the two previous figures, but for a potential structure consisting of two identical barriers of heigth 6 a.u., of width 1 a.u. and separated by a well 12 a.u. wide. This potential is shown in Fig. 1. The field amplitude

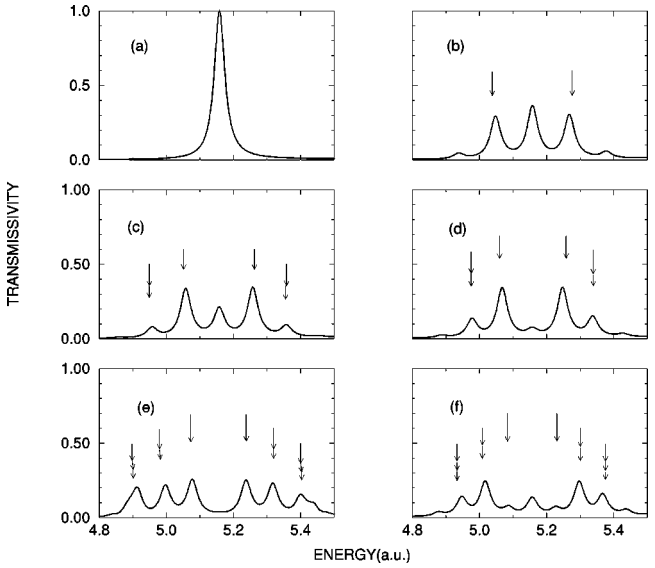

FIG. 6. Effect of a change of frequency on a multiplet. The electric field amplitude is $E_0=0.005$ a.u. The two barriers are of height 6 a.u. and of width 1 a.u. The intermediate well has a width of 12 a.u. [cf. Fig. 1(c)]. Only the total tranmissivity is shown. (a) The field-free transmission in the region of a resonance of energy $E_R=5.158-i0.019$ a.u. The frequencies are 0.11, 0.10, 0.09, 0.08, and 0.07 a.u. in panels (b)–(f), respectively. *n*-headed arrows are at positions $E_R \pm n\omega$.

is in all cases $E_0=0.005$ a.u. The frequency takes the values 0.11, 0.10, 0.09, 0.08, and 0.07 a.u. Figure 6(a) displays the field-free transmissivity close to a resonance of energy $5.158-i0.019$ a.u. As the frequency decreases (i.e., as the frequency gets closer to the width), the transfer of transmissivity away from the center operates again. This shows in a different way that the central part of the spectrum can disappear because of either a lower frequency or a higher coupling, two parameters which oppose transmission at the original resonance position.

V. APPLICATION TO A BIASED DOUBLE-BARRIER POTENTIAL

We now turn to an example related to resonant tunneling in semiconductor devices that was alluded to in the introductory section. The pioneering work is that of Tsu and Esaki [14] who predicted that the characteristics of a double-barrier structure should be nonlinear. This was very soon confirmed experimentally [21]. The power of the transfer-matrix method can be demonstrated in this situation since, although a stepwise constant potential results at first from the growth of an heterostructure, tunneling of an electron is induced by the application of a static electric field. For critical values of this field the distortion of the double barrier is such as to bring one of the resonant energies in coincidence with the energy of the incoming electron.

Our model is built with parameters met in such devices. Two barriers of width 20 Å or 37.79 a.u. are separated by a well of width 50 Å or 94.48 a.u. The height of the barriers is 1 eV or 0.03675 a.u. The effective mass of the electron is 0.1 a.u. We will consider coupling to a field of frequency $\omega=45$ meV or 0.001 654 a.u., typical of the frequency of lon-

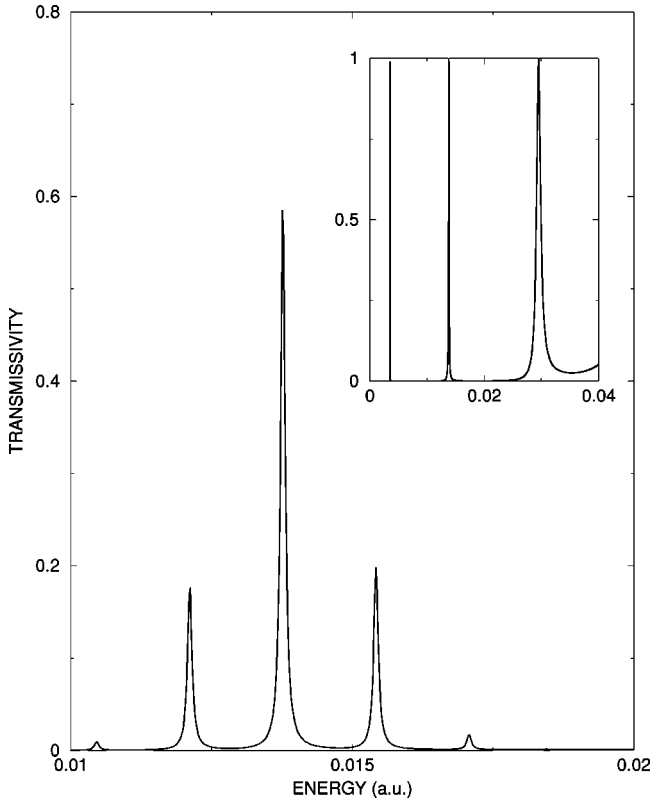

FIG. 7. Transmissivity of a double-barrier structure with coupling of an incident electron of effective mass 0.1 a.u. to an oscillatory field. Two barriers of widths 20 Å are separated by a well of width 50 Å. The height of the barriers is 1 eV. The frequency is $\omega=45$ meV and the maximum field amplitude $E_0=0.000\,005$ a.u. The transmissivity is shown as a function of the incident energy in the neighborhood of the second of the three field-free resonances displayed in the inset.

gitudinal optical phonons [9]. The oscillatory electric field has an amplitude $E_0=0.000\,005$ a.u. so as to produce a coupling W with an order of magnitude compatible with the other energies present in the model. The product of the electric field amplitude by the overall length of the structure gives for W 0.000 85 a.u. or 0.023 eV. Although the formalism implies consideration of an oscillatory electric field, it is only a matter of interpretation of the coupling parameter to view it as involving a one-mode phonon field. The wave equation in length gauge derived from Eq. (1) gives $E_0 x \sin(\omega t)$ for the coupling to the field. A bilinear coupling to a one-mode phonon field would be of the form $\gamma x(a\dagger + a)$. With a time periodic Hamiltonian, a coupling involving $\sin(\omega t)$ has the same effect as $(a\dagger + a)$, which is to produce a change in the energy of the field by $\pm\omega$. Our Hamiltonian is therefore a simplified version of that used in Refs. [11] and [22] to study the effect of electron-phonon interaction on resonance tunneling.

Figure 7 gives the transmissivities in the absence of a static field. In the inset the transmissivity of the double barrier shows that three resonances exist in the well at energies 0.003 52, 0.0138, and 0.0295 a.u. After coupling to the oscillatory field, two satellite peaks appear on both sides of the second resonance at the expense of the central peak. The peaks on the left or the right are essentially of either T_1 or T_{-1} character. We turn now to Fig. 8. The transmissivities

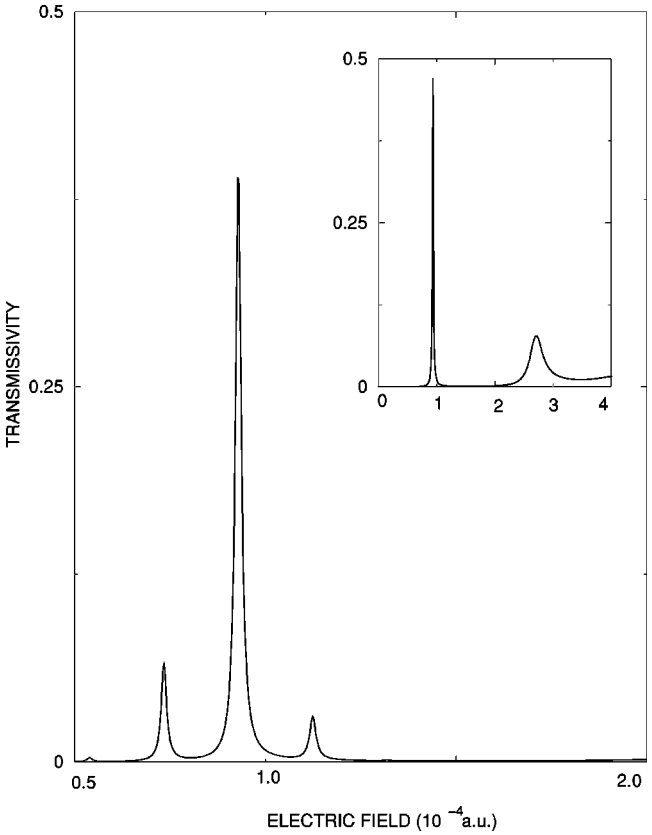

FIG. 8. A bias potential is applied to distort the potential structure studied in Fig. 7. An example of this distortion is shown Fig. 1(d). The oscillatory field is the same. Transmissivity is given as a function of the amplitude of the static electric field at a fixed incident energy (0.005 52 a.u.), intermediate between the first two resonances of the field-free case (inset of Fig. 7). Replicas appear on both sides of the resonance, which are due to either absorption (left peak), or emission (right peak). Inset: with no oscillatory field there are two values of the static electric field amplitudes that bring the two upper resonances of the distorted double barrier in coincidence with the incident energy.

are shown as a function of an applied bias static field. The potential is no longer stepwise constant and is different for every value of the bias field. Figure 1(d) gives an example belonging to this set of potentials. It is simulated by 100 steps. A check of the results versus the number of steps has shown that this is appropriate for the case at hand. The calculations are done at fixed energy taken equal to 0.005 52 a.u., that is intermediate between the two resonances of the inset of Fig. 7. The inset of Fig. 8 shows that as the amplitude of the static field increases, the second and third resonances of the deformed double barrier pass successively at the fixed energy. This occurs for amplitudes of the field equal to 0.000 093 and 0.000 27 a.u. The maximum transmissivities are far from unity, in constrast with the field-free case. This is due to the asymmetry of the double-barrier induced by the static field. The corresponding bias voltages are, respectively, 0.43 and 1.25 V. Finally when both static and oscillatory electric fields are present, we observe again a satellite structure. The second resonance of the inset is examined. We note that the left peak, corresponding to the T_1 process would not be present if, in the absence of any bias, the fixed energy is between $E_R-\omega$ and E_R, with E_R being a resonance energy of the well.

It is to be stressed that the ability to introduce an arbitrary potential in the study of resonance tunneling, with the electron coupled to an oscillating field, may be useful in the optimization of the parameters of a given device, for instance to enhance a satellite resonance. There is a great flexibility in the design of semiconductor heterostructures: the widths and heights of the rectangular barriers can be varied almost at will in a layer of the material $Al_xGa_{1-x}As$. It is even possible, by grading x to produce a barrier or a well of a desired shape [23]. It would be also useful to investigate how the transmissivity is affected if the changes in effective masses are taken into account. It is known [24] that this effect destroys the unit transmissivity which is the signature of certain symmetric or asymmetric structures. The modification to take into account the local character of the effective mass [25] is a minor one in a transfer-matrix technique.

VI. CONCLUSION

We have shown on a number of examples ranging from the rectangular barrier to the biased double-barrier potential that the transfer-matrix approach with inclusion of a coupling to an oscillatory field has considerable flexibility. Most potentials have to be treated through knowledge of their values at a set of points on a grid. The representation as a sequence of stepwise constant potentials is therefore common practice and the present method is applicable. Accurate calculations in the case of the double-barrier potential give clear evidence that some drastic changes in the transmissivity occur either when the coupling to the field increases, or when the frequency decreases. In both cases transmission at the energy of the field-free resonance is inhibited. This corroborates and extends previous analysis based on approximate treatments.

Extensions to situations with a more complicated geometry (for instance tunnelling of an electron between two quantum dots) can be envisaged if there is the possibility of eliminating all coordinates except the reaction coordinate. This elimination leads generally, in the absence of the field, to a set of coupled equations. Transfer-matrix algorithms have been formulated for such a situation [26]. In the presence of the field there will be a set of Gordon-Volkov waves for each channel. The matching technique should be very similar to that developed in the present work.

ACKNOWLEDGMENTS

R. L. thanks Professor N. Moiseyev for stimulating discussions and hospitality in his group at Technion, Haifa, Israel. C. P. V. thanks the Basque Government for financial assistance. We acknowledge a grant of computing time from Institut du Développement et des Ressources en Informatique Scientifique (IDRIS) under Project No. 980425.

[1] D. G. Sokolovski and M. Yu. Sumetski, Theor. Math. Phys. **64**, 802 (1985).
[2] D. Sokolovski, J. Phys. C **21**, 639 (1988).
[3] D. Sokolovski, Phys. Rev. B **37**, 4201 (1988).
[4] M. Ya. Azbel, Phys. Rev. Lett. **68**, 98 (1992).
[5] M. Ya. Azbel, Europhys. Lett. **18**, 537 (1992).
[6] M. Ya. Azbel, Phys. Rev. B **46**, 7596 (1992).
[7] M. Ya. Azbel and V. M. Tsukernik, Europhys. Lett. **41**, 7 (1998).
[8] M. Büttiker and R. Landauer, Phys. Rev. Lett. **49**, 1739 (1982).
[9] V. J. Goldman, D. C. Tsui, and J. E. Cunningham, Phys. Rev. B **36**, 7635 (1987).
[10] C. Zhang, M. L. F. Lerch, A. D. Martin, P. E. Simmonds, and L. Eaves, Phys. Rev. Lett. **72**, 3397 (1994).
[11] N. S. Wingreen, K. W. Jacobsen, and J. W. Wilkins, Phys. Rev. Lett. **61**, 1396 (1988).
[12] N. Zou and K. A. Chao, Phys. Rev. Lett. **69**, 3224 (1992).
[13] R. A. Sacks and A. Szöke, Phys. Rev. A **40**, 5614 (1989).
[14] R. Tsu and L. Esaki, Appl. Phys. Lett. **22**, 562 (1972).
[15] B. Ricco and M. Ya. Azbel, Phys. Rev. B **29**, 1970 (1984).
[16] D. J. Fischer and C. Zhang, J. Appl. Phys. **76**, 606 (1994).
[17] K. F. Brennan and C. J. Summers, J. Appl. Phys. **61**, 614 (1987).
[18] M. G. Rozman, P. Reineker, and R. Tehver, Phys. Rev. A **49**, 3310 (1994).
[19] D. K. Ferry and S. M. Goodnick, *Transport in Nanostructures* (Cambridge University Press, Cambridge, 1997).
[20] E. Merzbacher, *Quantum Mechanics* (Wiley, New York, 1970), Chap. 6.
[21] L. L. Chang, L. Esaki, and R. Tsu, Appl. Phys. Lett. **24**, 593 (1974).
[22] W. Cai, T. F. Zheng, P. Hu, B. Yudanin, and M. Lax, Phys. Rev. Lett. **63**, 418 (1989).
[23] S. Sen, F. Capasso, A. C. Gossard, R. A. Spah, A. L. Hutchinson, and S. N. G. Chu, Appl. Phys. Lett. **51**, 1428 (1987).
[24] C. J. Arsenault and M. Meunier, Phys. Rev. B **39**, 8739 (1989).
[25] G. Bastard, Phys. Rev. B **24**, 5693 (1981).
[26] M. V. Basilevsky and V. M. Ryaboy, Chem. Phys. **41**, 461 (1979).